

## Dynamic Cr(III) uptake by *Macrocystis pyrifera* and *Undaria pinnatifida* biomasses

Josefina Plaza Cazón<sup>1</sup> · Marisa Viera<sup>1</sup> · Edgardo Donati<sup>1</sup> ✉

<sup>1</sup> Universidad Nacional de La Plata, Facultad de Ciencias Exactas, Centro de Investigación y Desarrollo en Fermentaciones Industriales, La Plata, Argentina

✉ Corresponding author: donati@quimica.unlp.edu.ar  
Received November 30, 2012 / Invited Article  
Published online: May 15, 2013  
© 2013 by Pontificia Universidad Católica de Valparaíso, Chile

### Abstract

**Background:** The increased industrial activity has resulted in the discharge of large amount of pollutants including non-degradable metals into the environment. Chromium is produced in several industrial processes and it can be found in the environment in two stable oxidation states, Cr(VI) and Cr(III). Cr(VI) is more hazardous due to its carcinogenic and mutagenic effects on living organisms. Although much less toxic, Cr(III) can also exert genotoxic effects under prolonged or severe exposure. It can be separated from the solution by precipitation but biosorption using brown algae seems to be an effective and sustainable treatment technique owing to its cost-effectiveness and environmental friendly characteristics. *Macrocystis pyrifera* and *Undaria pinnatifida* are two marine brown macroalgae with high capability of removing heavy metals including Cr(III) in batch mode of operation. In this work packed bed biosorption of Cr(III) by *M. pyrifera* and *U. pinnatifida* biomasses was evaluated.

**Results:** The shapes of the breakthrough curves were rather different for each biomaterial. Parameters like the breakthrough time ( $t_b$ ) and zone mass transfer (MTZ) showed that *U. pinnatifida* has greater affinity for Cr(III). The maximum adsorption capacity at the exhaustion operating time ( $t_e$ ) demonstrated that *M. pyrifera* has higher retention capacity of Cr(III). The experimental data were fitted to Thomas, Yoon-Nelson and Dose-Response models. The best correlation coefficient (0.94 or 0.96) was obtained with Dose-Response that accurately describes the uptake behaviour of Cr(III) on the seaweed biomasses under different experimental conditions. The FT-IR spectra evidenced that Cr(III) adsorption occurred mainly by interaction between metal and carboxylate groups present on both the seaweed surfaces.

**Conclusions:** *M. pyrifera* and *U. pinnatifida* biomasses are efficient biosorbents for Cr(III) adsorption under a continuous mode of operation although differences between uptake capacities suggest different mechanisms involved in the biosorption.

**Keywords:** biosorption, brown algae, chromium, heavy metals.

### INTRODUCTION

The increased industrial activity has resulted in the discharge of large volume of pollutants into the environment. Unlike most organic contaminants, metals are more hazardous since they are not biodegradable and can be accumulated in living organisms and transferred throughout the food chain (Amuda et al. 2007). Among the more prominent heavy metal contaminants is chromium, a metal commonly used in electroplating, leather tanning, textile dyeing, metal processing and wood preservation (Sari et al. 2007; Pérez Marín et al. 2009). Chromium can be found in the environment in two stable oxidation states, Cr(VI) and Cr(III). Cr(VI) compounds are highly soluble in water and very

toxic to aquatic organisms; these compounds can pass through cell membranes and interact with DNA and cell proteins generating carcinogenic and mutagenic effects (Arica et al. 2005).

Trivalent chromium is up to one hundred times less toxic than hexavalent chromium. That is why current conventional methods for treating Cr(VI) generally consist of reduction to Cr(III) which in addition is less soluble and can be separated from the solution by precipitation with alkali. However, Cr(III) is lightly soluble even in not so acidic solutions. Although Cr(III) is recognized as an essential nutrient required for the metabolism of sugars and fats, it can exert genotoxic effects under prolonged or severe exposure (Eastmond, 2012). In water Cr(III) is toxic to fish when its concentration exceeds  $5.0 \text{ mg} \times \text{L}^{-1}$ . The maximum allowable limit for Cr in drinking water considered safe by the US Environmental Protection Agency is  $0.1 \text{ mg} \times \text{L}^{-1}$ , although the World Health Organisation sets the upper limit at  $0.01 \text{ mg} \times \text{L}^{-1}$  (Pérez Marín et al. 2009). In addition it can be oxidized by microorganisms or other chemical compounds in the environment.

Among chemical precipitation there are other methods for Cr(III) removal although biosorption has been suggested as an effective and sustainable treatment technique owing to its cost-effectiveness and environmental friendly characteristics. The possibility of using dead biomass or products of their metabolism overcomes problems of toxicity and even allows the regeneration and reuse of biomaterial for several successive cycles of sorption-desorption (Plaza Cazón et al. 2012a). Many biological materials (bacteria, fungi, yeast, algae, agro-industrial wastes) have been studied as biosorbents (Bueno et al. 2008; Murphy et al. 2008; Ulüozlü et al. 2008; Pérez Marín et al. 2009) but brown seaweeds are extensively used for metal biosorption due to their high uptake capacities; in addition they are abundant and easily available (Davis et al. 2003; Murphy et al. 2008). *Macrocystis pyrifera* and *Undaria pinnatifida* are two marine brown macroalgae (*Phaeophyceae*) frequently found in the south coast of Atlantic Ocean. *M. pyrifera* is a native species broadly distributed in Argentina from Chubut to Tierra del Fuego and used as raw material for cattle feed additives and for producing fertilizers and alginic acid (Boraso and Zaixo, 2012). Frequently, big amounts of this species are deposited on the beach of Bahía de Camarones causing unpleasant odours and a negative impact on local tourism. The invasive species *U. pinnatifida* was detected at Puerto Madryn in 1992 and today it is spread along more than 1,000 km of the Patagonic coast (Martin and Cuevas, 2006). *U. pinnatifida* species reaches the macroscopic sporophytic phase during winter and dies in summer. Dense kelp forests of this species finally arrive to the coast in summer provoking a negative impact on tourism. Also, recent studies have shown an adverse effect on native macroalgal assemblages and reef fish (Dellatorre et al. 2012).

We have recently published some papers using such seaweeds for removing different metals from aqueous solutions; *M. pyrifera* and *U. pinnatifida* showed high Cr(III) uptake in batch studies (Plaza Cazón et al. 2011; Plaza Cazón et al. 2012a; Plaza Cazón et al. 2012b). Most biosorption studies deal with batch systems because of a simpler experimental design to determine optimal operating conditions (pH, pretreatment, particle size, contact time, etc.). However, practical applications of metal removal imply the use of continuous systems (generally packed bed columns) for the investigation of both equilibrium and kinetic performance; in addition, continuous systems constitute a suitable approach to industrial applications. The dynamic biosorption of metals ions can be interpreted analyzing the shape and position of the breakthrough curves. Quantitative prediction of the performance of packed-bed columns involves prediction of those characteristics of the breakthrough curve. If the breakthrough curves can be reliably predicted using laboratory measurements, studies at pilot plant scale before the industrial applications could be obviated. Quantitative prediction implies the application of appropriate mathematical modeling techniques which are generally complex and require rigorous resolution methods. Instead of them, simpler models such as Thomas, Yoon and Nelson, BDST and Dose-Response models, can be used to approach the behaviour of the uptake process taking place in the column biosorption process.

The main aim of this work was to evaluate the Cr(III) biosorption in a fixed bed columns filled with *M. pyrifera* and *U. pinnatifida* biomasses. Results were described using Thomas, Yoon-Nelson and Dose-Response models. Fourier transform infrared spectroscopy (FT-IR) was employed to identify the functional groups involved in the binding of Cr(III) to those seaweed biomasses.

## MATERIALS AND METHODS

### Biological material: pre-treatment

Algae biomasses were ground and sieved and the 10-16 mesh (*i.e.*, 1.18-2 mm) particle size fraction was selected, washed several times with distilled water and dried at 50°C. Some organic material can be leached from the biomass during the sorption process; these organic compounds could cause the precipitation or the complexation of chromium ions affecting the sorption properties of the biomasses. To prevent such leaching, biomasses were treated with 0.2 M CaCl<sub>2</sub> at pH 5.0 for 24 hrs. Then biomasses were repeatedly washed with distilled water and dried as mentioned before.

### Adsorption and desorption of Cr(III) in packed bed columns

Studies were carried out using a glass column of 2.5 cm in inner diameter and 15 cm in length. The void volume of the packed column was 65 mL. Two columns were packed with 5.210 g of each biomaterial separately, yielding *M. pyrifera* and *U. pinnatifida* biomass beds of approximately 8 and 6 cm respectively. At the top and at the base of the column, a layer of glass wool was placed to prevent clogging of the inlet or outlet piping. Cr(III) concentration and pH value were selected from previous results in batch studies in order to avoid possible Cr(III) precipitation (it occurs at pH 4.6 when the total concentration was 100 mg/L). The procedure was the following: firstly distilled water was pumped to avoid a sudden initial increase in the metal initial concentration due to a rapid absorption of water by the dried seaweed. 50 mg x L<sup>-1</sup> Cr(III) solutions at pH 4.0 were fed upward through the column at 100 mL x h<sup>-1</sup> using a peristaltic pump (Watson Marlow 101 U/R). This procedure was adequate to allow the homogeneous contact between the solution and the biosorbent preventing the formation of preferential channels. Effluent was collected from the top of the column to determine metal, calcium, and sodium concentrations and pH measurement. At the end of the experiment, 500 mL of distilled water was pumped into the column to remove any residual metal ions. Then the biomasses were collected and washed with distilled water, dried for 24 hrs at 50°C, and stored for desorption experiments. Desorption studies were also carried out in dynamic systems. Loaded-biomass (4.43 ± 0.10 g) from dynamic adsorption experiments was packed into the column. The eluent, 0.1M HNO<sub>3</sub>, was fed upward at 100 mL x h<sup>-1</sup>. The effluent was collected from the top of the column at different times and metal concentration and pH were measured.

### Analytical methods

All the experiments were carried out in duplicate and samples were filtered through 0.45 µm membrane. An atomic absorption spectrophotometer Shimadzu AA6650 (Shimadzu Corporation Kyoto, Japan) was used to measure metal concentrations at the beginning, at the end and at different times in the biosorption and desorption experiments. FT-IR analyses were performed on a FT-IR spectrometer (Perkin Elmer) using KBr pellets (the fraction of sample was about 0.1% w/w).

The amount of metal ion adsorbed into the biosorbent in column experiments was calculated on the basis of experimental breakthrough curves using the following equation:

$$q_{column} = \int_{t=0}^{t=t_e} \left( \frac{C_0 - C}{m} \right) dt$$

[Equation 1]

where,  $C_0$  and  $C$  are the inlet and outlet metal ion concentration (mg x L<sup>-1</sup>),  $m$  is the mass of sorbent (g),  $t_e$  is the exhaustion operating time (h) (Wilson et al. 2012).

The total heavy metal mass fed into the column,  $m_{total}$  (mg) is calculated by the following equation:

$$m_{total} = \frac{C_0 Q t_e}{1000}$$

[Equation 2]

where  $Q$  is the volumetric flow rate ( $\text{mL} \times \text{h}^{-1}$ ).

Also, the breakthrough curve allowed calculating others parameters, such as the mass transfer zone (MTZ) (Lee et al. 2008):

$$MTZ = L \left( \frac{t_e - t_b}{t_e} \right)$$

[Equation 3]

where  $t_b$  is the breakthrough time (h) and  $L$  is the total packed bed height (cm).

The results from continuous assays were fitted employing the equation models presented in Table 1.

**Table 1. Equations applied for the analysis of the experimental results from dynamic experiments.**

| Model           | Integrated equation  | Reference                  |
|-----------------|--|----------------------------|
| Thomas          | $\frac{C}{C_0} = \frac{1}{1 + \exp \left[ \frac{k_{Th}}{Q} (q_0 m - C_0 V_{eff}) \right]}$ | (Senthilkumar et al. 2006) |
| Yoon and Nelson | $\ln \left( \frac{C_0}{C} - 1 \right) = k_{YN} \tau - k_{YN} t$                            | (Senthilkumar et al. 2006) |
| Dose-response   | $\frac{C}{C_0} = 1 - \frac{1}{1 + \left( \frac{C_0 V_{eff}}{q_0 m} \right)^a}$             | (Senthilkumar et al. 2006) |

The quantity of metal stripped out of the column in the desorption experiments was calculated by the equation (Zhang and Banks, 2006):

$$m_d = \sum C_i v_i$$

[Equation 4]

where  $m_d$  is the metal stripped out of the column,  $C_i$  is the effluent metal concentration at the  $i$  fraction,  $v_i$  is the fraction  $i$  volume. The desorption ratio ( $D.R$ ) was calculated from the mass of metal ions desorbed and the total mass of metal loaded in the biomass using the following equation (Zhang and Banks, 2006):

$$D.R = \frac{m_d}{m_l} 100$$

[Equation 5]

## RESULTS AND DISCUSSION

The efficiency of the columns was evaluated through the analysis of the breakthrough curves, where the  $C/C_0$  is plotted vs. the operating time or the effluent volume. The resulting breakthrough curves obtained when the packed bed columns filled with *M. pyrifera* and *U. pinnatifida* biomasses were fed with Cr(III) solution are shown in Figure 1. Table 2 presents the parameters obtained through the analysis of the breakthrough curves and the application of Thomas, Yoon-Nelson and Dose-Response models (Table 1). The breakthrough time ( $t_b$ ) is the time for complete metal recovery (full efficiency of the sorbent), and the exhaustion operating time ( $t_e$ ) is the time corresponding to full use of the sorbent. Cr(III)  $t_b$  corresponding to *M. pyrifera* biosorbent (6 hrs) is lower than for *U. pinnatifida* (25 hrs). These results indicate a much higher affinity of *U. pinnatifida* biomass for Cr(III). However they do not fit with Langmuir affinity coefficients for Cr(III) adsorption on both biomasses reported in a previous paper (Plaza Cazón et al. 2012a) which were similar to each other (1.20 L.mmol<sup>-1</sup> for *M. pyrifera* and 1.06 L.mmol<sup>-1</sup> for *U. pinnatifida*).

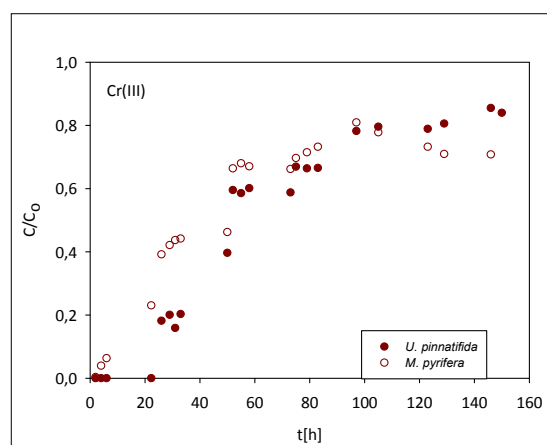


Fig. 1 Cr(III) breakthrough curves in fixed bed column packed with calcium-treated *M. pyrifera* and *U. pinnatifida* biomasses.

The mass transfer zone (MTZ) is another parameter frequently used to examine the effective height of a sorption column. MTZ is the active part of the fixed bed where adsorption actually takes place. The lower the MTZ length, the closer the system is to ideality (step function). This means that short MTZ represents systems with high removal efficiency (Kleinübing et al. 2011). In the present case, MTZ were 7.0 cm (87.5%) and 5.2 cm (86.66% for Cr (III)-loaded column filled with *M. pyrifera* and *U. pinnatifida* biomasses, respectively. This is an indication that *U. pinnatifida* shows greater affinity than *M. pyrifera*.

Cr(III) uptake in the column at saturation ( $q$ ) was greater than Cr(III) uptake ( $q_m$ ) in batch studies and very close to the values of maximum Langmuir adsorption capacity ( $q_m$ ) obtained in batch assays. This may be due to the continuous formation of a large concentration gradient at the interface zone during column operation, which is the driving force for the adsorption process. Instead, such concentration gradient decrease with time in batch adsorption (Gupta et al. 2004). Values of  $t_b$  calculated according to Thomas model were lower than those obtained from the curves (Table 2). Moreover this model gave values of  $q_0$  lower than those obtained from experimental data. All these facts confirm that the Thomas model underestimates the performance of the process at the beginning of the operation as it has been

previously reported (Calero et al. 2009). The values of  $\tau$  (the time required to adsorb 50% of the initial concentration) determined from experimental data using Yoon and Nelson model were 41.63 hrs and 59.87 hrs for *M. pyrifera* and *U. pinnatifida* biomasses, respectively. The correlation coefficients found for the three models are in general acceptable; however, the Dose-Response model gave the best fitting to the experimental data in all the measured range ( $R^2$  was 0.94 and 0.96) as shown in Table 2.

**Table 2. Breakthrough curve, Thomas, Yoon-Nelson and Dose-Response models parameters for Cr(III) uptake using fixed bed columns with *M. pyrifera* and *U. pinnatifida* biomasses.**

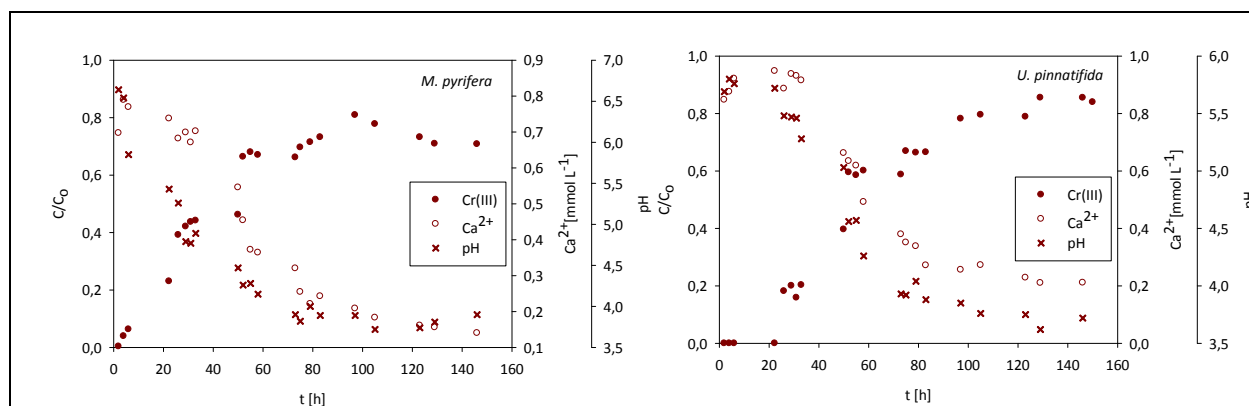
| Parameters         |   | <i>M. pyrifera</i>     | <i>U. pinnatifida</i>  |
|--------------------|---|------------------------|------------------------|
| Breakthrough curve | Q [mL x h <sup>-1</sup> ]                               | 120                    | 100                    |
|                    | t <sub>b</sub> [h]                                      | 6                      | 25                     |
|                    | t <sub>e</sub> [h]                                      | 146                    | 150                    |
|                    | V [mL]  | 720                    | 2500                   |
|                    | q <sub>0</sub> [mmol x g <sup>-1</sup> ]                | 3.22                   | 2.7                    |
|                    | MTZ [cm]  | 7.0                    | 5.2                    |
|                    | m <sub>total</sub> [mg]                                 | 884.40                 | 740.4                  |
|                    | % ads.  | 42.62                  | 46.58                  |
| Thomas             | K <sub>Th</sub> [L.mg <sup>-1</sup> x h <sup>-1</sup> ] | 5.7 x 10 <sup>-4</sup> | 4.2 x 10 <sup>-3</sup> |
|                    | q <sub>0</sub> [mmol x g <sup>-1</sup> ]                | 1.10                   | 1.11                   |
|                    | R <sup>2</sup>  | 0.87                   | 0.95                   |
|                    | t <sub>b</sub> [h]                                      | 51.6                   | 12.7                   |
|                    | t <sub>e</sub> [h]                                      | 76                     | 55.6                   |
|                    | MTZ [cm]  | 6.3                    | 6.7                    |
| Yoon Nelson        | K <sub>YN</sub> [h <sup>-1</sup> ]                      | 0.0183                 | 0.0314                 |
|                    | $\tau$ [h]  | 41.63                  | 59.87                  |
|                    | R <sup>2</sup>  | 0.83                   | 0.87                   |
| Dose Response      | q <sub>0</sub> [mmol x g <sup>-1</sup> ]                | 0.89                   | 1.01                   |
|                    | R <sup>2</sup>  | 0.94                   | 0.96                   |

The release of Ca(II) and the pH behaviour were also evaluated during column operation. At the beginning of the assays pH of the inlet solution was 4. When this solution flooded the column the pH increased to 6-7 probably due to the dilution; as indicated above, the biomass was in contact with distilled water for avoiding the sudden water adsorption. Later the pH decreased and when the biomasses seemed to be saturated the pH reached a value close to the inlet pH (Figure 2). Similar behaviour was reported for Cr(III) adsorption by olive stones (Calero et al. 2009).

As shown in Figure 2, the release of Ca(II) increased significantly before the t<sub>b</sub> for each metal and then it remained constant when the column began to be saturated. The calcium present on the surface of the algal cell wall due the pretreatment applied was displaced by the heavy metal during the biosorption process. Its release varies according to the heavy metal involved in the process: this suggests that ion exchange contributes to the biosorption of Cr(III) on both biomaterials. Besides calcium, also sodium and potassium were also released during Cr(III) adsorption while there was insignificant proton release. However, the balance between released and adsorbed ions was quite different for each biomass. Considering that at pH 4 more than 80% of dissolved species in a Cr(III) solution are Cr<sup>3+</sup> and CrOH<sup>2+</sup>, the milliequivalents adsorbed were almost equal to the milliequivalents released in the case of *U. pinnatifida*. However, in the case of *M. pyrifera*, the milliequivalents adsorbed were no more than 70-80% of the milliequivalents of released ions. These differences suggest different adsorption mechanisms operating in each case.

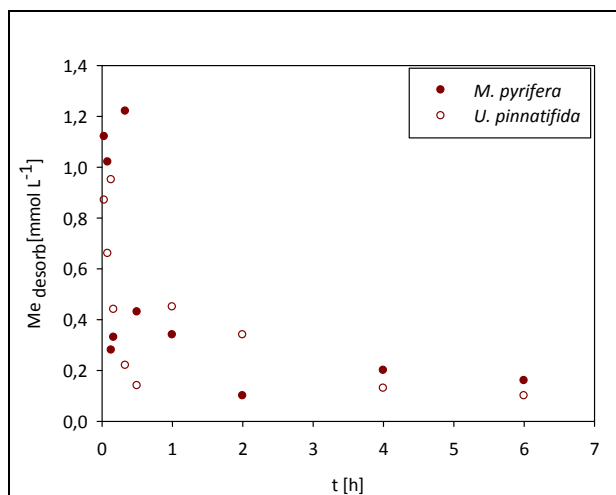
In order to assess their reusability (*i.e.*, regeneration of the biosorbent allowing its successive use) Cr(III) loaded-biomasses recovered from columns were used in desorption columns using 0.1 M HNO<sub>3</sub>

as eluent. This eluent was chosen since high metal (Zn, Cd, and Ni) recoveries have been obtained from these biomasses using mineral acid treatments, especially with 0.1 M  $\text{HNO}_3$  (Plaza Cazón et al. 2012b). Also, eluting with EDTA at the same concentration allowed similar recoveries but ESEM micrographs showed that the structure of the cell has been strongly deteriorated by the treatment. This effect was not observed when the biomass was in contact with  $\text{HNO}_3$  except at concentrations higher than 0.1 M.



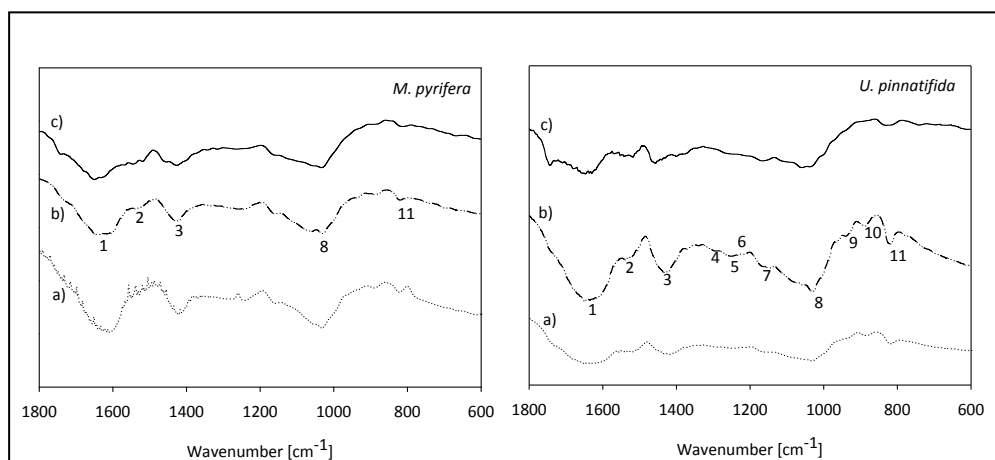
**Fig. 2** Cr(III) breakthrough curves for calcium-treated *M. pyrifera* and *U. pinnatifida* biomasses. Empty and closed circle symbols represent calcium release and Cr(III) concentration in the eluate, respectively, while cross symbols indicate pH behaviour during Cr(III) uptake.

Figure 3 shows Cr(III) released during the desorption column operation. The maximum desorption capacity was obtained in less than one hour. The desorption percentages obtained for Cr(III) were 2.7% and 24.8% achieved in *M. pyrifera* and *U. pinnatifida* loaded desorption columns, respectively. The low Cr(III) recovery yield by an acid like  $\text{HNO}_3$  suggests that Cr(III) ion was not easily replaced by protons and the contribution of ion exchange in the adsorption mechanism was minor; as it occurred during the Cr(III) adsorption, it is even more so in the case of *M. pyrifera*. Many authors refer to complete or almost complete recovery of metals from biosorbents using mineral acid treatments. In the case of Cr(III) desorption, the reports are contradictory: although some authors report high Cr(III) recoveries using  $\text{HNO}_3$  from different biosorbents like bacterial biomass (Yahya et al. 2012) and blue-green algae *Spirulina* sp (Chojnacka et al. 2005), most reports indicate very low Cr(III) desorption using  $\text{HNO}_3$  or other mineral acids in the case of *Chlorella miniata* biomass (Han et al. 2006), agro-waste materials (García-Reyes et al. 2009), *S. cerevisiae* biomass (Ferraz et al. 2004), and *S. neglecta* biomass (Singh et al. 2012). However, it is widely accepted that Cr(III) desorption occurs to a lesser extent than in other common heavy metals, like Cd, Ni, Cu, Zn or Pb, independent from the type of biosorbent. This suggests that the binding mechanism operating in Cr(III) adsorption is probably different and binding is stronger. Among several mechanisms, ion exchange seems to be the most important process for metal adsorption on algal biomass; in such case, protons (or eventually calcium ions) compete with metal ions for the binding sites and replace them if the concentration of desorbing agent is high enough. That is why ion exchange mechanism should be reversible and the biosorbed metal should be recovered by acid washing.



**Fig. 3** Cr(III) desorption column packed with loaded- *M. pyrifera* and *U. pinnatifida* biomasses.

Many functional groups on the surface of the biomass may contribute to metal uptake. FT-IR analysis allowed identifying the chemicals groups on the surface of the biomasses; Figure 4 shows the FT-IR spectra of both biomasses restricted for the wavenumber range where most of the active groups involved in the sorption of metals may be detected; in the same figure, spectra of untreated biomasses, biomasses treated with  $\text{CaCl}_2$  and biomasses after contact with Cr(III) have been included. As seen in this figure and explained in the legend, carboxylic, amide and alcohol groups were detected in both biomasses. However, the spectra for *U. pinnatifida* biomass was more complex and other peaks, especially those corresponding to sulphonate groups, could be detected.



**Fig. 4** FT-IR spectra of *M. pyrifera* and *U. pinnatifida* biomasses. (a) Biomasses at pH 4 without Cr(III); (b) control; (c) Cr(III)-loaded biomasses at pH 4. Peaks marked for *M. pyrifera* and *U. pinnatifida*, respectively: (1) 1622 and 1639  $\text{cm}^{-1}$ : C=O (in carboxylate) strong asymmetric stretching; (2) 1520 and 1524  $\text{cm}^{-1}$ : C-O in amides; (3) 1424 and 1429  $\text{cm}^{-1}$ : N-H bending and symmetric  $\text{COO}^-$  stretching; (4) 1338 and 1338  $\text{cm}^{-1}$   $\text{SO}_3$  asymmetric; (5) n.d. and 1297  $\text{cm}^{-1}$ : C=O symmetric stretching; (6) n.d. and 1249  $\text{cm}^{-1}$ : CN stretching and COOH bending; (7) n.d. and 1216  $\text{cm}^{-1}$ : COOH bending; (8) n.d. and 1148  $\text{cm}^{-1}$ :  $\text{SO}_3$  symmetric; (9) 1033 and 1027  $\text{cm}^{-1}$ : C-O in alcohols; (10) n.d. and 941  $\text{cm}^{-1}$ : S-C in sulfonate groups; (11): 890 and 894  $\text{cm}^{-1}$ : C-H; 826 and 823  $\text{cm}^{-1}$ : C-H. n.d: Not detected.

According to the pH value used in the experiments, mostly carboxyl groups should participate in metal ions binding. By using potentiometric titrations and FT-IR analyses, Yun et al. (2001) demonstrated that the carboxyl groups in brown seaweed *Ecklonia* sp. biomass were the chromium-binding sites. Similarly Sawalha et al. (2007) showed that the trivalent chromium adsorption was mainly due to the



carboxyl groups of chemically modified saltbush biomass (*Atriplex canescens*). Results obtained in the present case support this fact: peaks corresponding to carboxylate groups were mostly modified after the contact with Cr(III).

The same functional group could take part in the adsorption of different metals, but through different mechanisms like ion-exchange, complexation and microprecipitation, among others. As indicated above, at pH 4 the dominant dissolved species in a Cr(III) solution are  $\text{Cr}^{3+}$  and  $\text{CrOH}^{2+}$ . Both species, together with protons and calcium ions, are strong acids reacting faster and forming stronger bonds with strong bases like carboxyl groups. That could explain why Cr(III) desorption is lower than Ni(II), Cu(II), and Zn(II) (borderline acids) and Cd (soft acid) which form weaker bonds with carboxyl groups. In addition, the formation of strong complexes can block the active sites making the adsorption almost irreversible by acid washing.

## CONCLUDING REMARKS

*M. pyrifera* and *U. pinnatifida* biomasses are efficient biosorbents for Cr(III) although the shape of Cr(III) breakthrough curves obtained for both materials were different. *M. pyrifera* had more capacity of Cr(III) adsorption than *U. pinnatifida*. The higher breakthrough time ( $t_b$ ) determined for *U. pinnatifida* meant a greater affinity for Cr(III) as supported by the MTZ values obtained. A good fit in all the experimental range was obtained by the Dose-Response model being adequate to predict the behaviour of Cr(III) uptake in the columns under other non-assayed experimental conditions. FT-IR analysis indicates that mostly carboxylate groups participated in Cr(III) adsorption process. The low Cr(III) recovery yield from the biomasses by  $\text{HNO}_3$  solution suggests that Cr(III) adsorption is not entirely reversible as ion exchange mechanism would imply and a stronger binding mechanism (complexation, for example) is likely to take place during adsorption.

## Nomenclature

$a$ : dose-response parameter  
 $C_0$ : inlet metal concentration ( $\text{mg} \times \text{L}^{-1}$  or mM)  
 $C$ : metal concentration ( $\text{mgL}^{-1}$  or mM)  
 $D.R.$ : desorbed rate (%)  
 $k_{Th}$ : Thomas rate constant ( $\text{mL} \times \text{min}^{-1} \times \text{mg}^{-1}$ )  
 $k_{YN}$ : Yoon-Nelson rate constant  
 $L$ : total height of packed bed (cm)  
 $m$ : mass of biosorbent (g)  
 $m_d$ : mass of metal stripped out of the column (mg)  
 $m_i$ : total heavy metal loaded in the biomass (mg)  
 $m_{total}$ : total metal mass sent to the column (mg)  
 $MTZ$ : mass transfer zone (cm)  
 $q_0$ : maximum solute capacity on the solid phase ( $\text{mg} \times \text{g}^{-1}$  or  $\text{mmol} \times \text{g}^{-1}$ )  
 $Q$ : flow rate ( $\text{mL} \times \text{h}^{-1}$ )  
 $q_{column}$ : capacity at exhaustion determine by the area below the breakthrough curve ( $\text{mg} \times \text{g}^{-1}$ )  
 $t_b$ : breakthrough time (h)  
 $t_e$ : exhaustion operating time (h)  
 $V$ : solution volume (L)  
 $V_{eff}$ : volume of metal solution passed through into column (mL)  
 $\tau$ : time required to reach 50% of total adsorption (on the breakthrough curve)

**Financial support:** This research work was supported by ANPCyT (PICT 339), CONICET (PIP 0368) and UNLP (X631).

## REFERENCES

- AMUDA, O.S.; GIWA, A.A. and BELLO, I.A. (2007). Removal of heavy metal from industrial wastewater using modified activated coconut shell carbon. *Biochemical Engineering Journal*, vol. 36, no. 2, p. 174-181. [\[CrossRef\]](#)
- ARICA, M.Y.; TÜZÜN, I.; YALCIN, E.; İNCE, Ö. and BAYRAMOGU, G. (2005). Utilisation of native, heat and acid-treated microalgae *Chlamydomonas reinhardtii* preparations for biosorption of Cr(VI) ions. *Process Biochemistry*, vol. 40, no. 7, p. 2351-2358. [\[CrossRef\]](#)

- BORASO, A. and ZAIXO, J.M. (2012). Algas marinas bentónicas. In: BOLTOVSKOY, D. ed. *Atlas de Sensibilidad Ambiental de la Costa y el Mar Argentino*. [cited 18 October 2012]. Available from Internet: <http://seaweedafrica.org/pdf/562DF4FA1149b1C475TSK191032E/48288.pdf>.
- BUENO, B.Y.M.; TOREM, M.L.; MOLINA, F. and DE MESQUITA, L.M.S. (2008). Biosorption of lead(II), chromium(III) and copper(II) by *R. opacus*: Equilibrium and kinetic studies. *Minerals Engineering*, vol. 21, no. 1, p. 65-75. [\[CrossRef\]](#)
- CALERO, M.; HERNÁNDEZ, F.; BLÁZQUEZ, G.; TENORIO, G. and MARTÍN- LARA, M.A. (2009). Study of Cr(III) biosorption in a fixed-bed column. *Journal of Hazardous Materials*, vol. 171, no. 1-3, p. 886-893. [\[CrossRef\]](#)
- CHOJNACKA, K.; CHOJNACKI, A. and GORECKA, H. (2005). Biosorption of  $\text{Cr}^{3+}$ ,  $\text{Cd}^{2+}$  and  $\text{Cu}^{2+}$  ions by blue-green algae *Spirulina* sp.: Kinetics, equilibrium and the mechanism of the process. *Chemosphere*, vol. 59, no. 1, p. 75-84. [\[CrossRef\]](#)
- DAVIS, T.A.; VOLESKY, B. and MUCCI, A. (2003). A review of the biochemistry of heavy metal biosorption by brown algae. *Water Research*, vol. 37, no. 18, p. 4311-4330. [\[CrossRef\]](#)
- DELLATORRE, F.G.; AMOROSO, R. and BARÓN, P.J. (2012). *El alga exótica Undaria pinnatifida en Argentina: Biología, distribución y potenciales impactos*. Editorial Académica Española, 60 p. ISBN 384845727X.
- EASTMOND, D.A. (2012). Factors influencing mutagenic mode of action determination of regulatory and advisory agencies. *Mutation Research/Reviews in Mutation Research*, vol. 751, no. 1, p. 49-63. [\[CrossRef\]](#)
- FERRAZ, A.I.; TAVARES, T. and TEIXEIRA, J.A. (2004). Cr(III) removal and recovery from *Saccharomyces cerevisiae*. *Chemical Engineering Journal*, vol. 105, no. 1-2, p. 11-20. [\[CrossRef\]](#)
- GARCIA-REYES, R.B.; RANGEL-MENDEZ, J.R. and ALFARO-DE LA TORRE, M.C. (2009). Chromium (III) uptake by agro-waste biosorbents: Chemical characterization, sorption-desorption studies, and mechanism. *Journal of Hazardous Materials*, vol. 170, no. 2-3, p. 845-854. [\[CrossRef\]](#)
- GUPTA, V.K.; MITTAL, A.; KRISHNAN, L. and GAJBE, V. (2004). Adsorption kinetics and column operations for the removal and recovery of malachite green from wastewater using bottom ash. *Separation and Purification Technology*, vol. 40, no. 1, p. 87-96. [\[CrossRef\]](#)
- HAN, X.; WONG, Y.S. and TAM, N.F.Y. (2006). Surface complexation mechanism and modeling in Cr(III) biosorption by a microalgal isolate, *Chlorella miniata*. *Journal of Colloid and Interface Science*, vol. 303, no. 2, p. 365-371. [\[CrossRef\]](#)
- KLEINÜBING, S.J.; DA SILVA, E.A.; DA SILVA, M.G.C. and GUIBAL, E. (2011). Equilibrium of Cu(II) and Ni(II) biosorption by marine alga *Sargassum filipendula* in a dynamic system: Competitiveness and selectivity. *Bioresource Technology*, vol. 102, no. 7, p. 4610-4617. [\[CrossRef\]](#)
- LEE, S.W.; PARK, H.J.; LEE, S.H. and LEE, M.G. (2008). Comparison of adsorption characteristics according to polarity difference of acetone vapor and toluene vapor on silica-alumina fixed-bed reactor. *Journal of Industrial and Engineering Chemistry*, vol. 14, no. 1, p. 10-17. [\[CrossRef\]](#)
- MARTIN, J.P. and CUEVAS, J.M. (2006). First record of *Undaria pinnatifida* (Laminariales, Phaeophyta) in Southern Patagonia, Argentina. *Biological Invasions*, vol. 8, no. 6, p. 1399-1402. [\[CrossRef\]](#)
- MURPHY, V.; HUGUES, H. and MCLOUGHLIN, P. (2008). Comparative study of chromium biosorption by red, green and brown seaweed biomass. *Chemosphere*, vol. 70, no. 6, p. 1128-1134. [\[CrossRef\]](#)
- PÉREZ MARÍN, A.B.; AGUILAR, M.I.; MESEGUER, V.F.; OTUÑO, J.F.; SÁEZ, J. and LLORENS, M. (2009). Biosorption of chromium(III) by orange (*Citrus cinensis*) waste: Batch and continuous studies. *Chemical Engineering Journal*, vol. 155, no. 1-2, p. 199-206. [\[CrossRef\]](#)
- PLAZA CAZÓN, J.; VIERA, M.; DONATI, E. and GUIBAL, E. (2011). Biosorption of mercury by *Macrocystis pyrifera* and *Undaria pinnatifida*: Influence of zinc, cadmium and nickel. *Journal of Environmental Sciences*, vol. 23, no. 11, p. 1778-1786. [\[CrossRef\]](#)
- PLAZA CAZÓN, J.; BENÍTEZ, L.; DONATI, E. and VIERA, M. (2012a). Biosorption of chromium(III) by two brown algae *Macrocystis pyrifera* and *Undaria pinnatifida*: Equilibrium and kinetic study. *Engineering in Life Science*, vol. 12, no. 1, p. 95-103. [\[CrossRef\]](#)
- PLAZA CAZÓN, J.; BERNARDELLI, C.; VIERA, M.; DONATI, E. and GUIBAL, E. (2012b). Zinc and cadmium biosorption by untreated and calcium-treated *Macrocystis pyrifera* in a batch system. *Bioresource Technology*, vol. 116, p. 195-203. [\[CrossRef\]](#)
- SARI, A.; TUZEN, M.; ULUÖZLÜ, Ö.D. and SOYLAK, M. (2007). Biosorption of Pb(II) and Ni(II) from aqueous solution by lichen (*Cladonia furcata*) biomass. *Biochemical Engineering Journal*, vol. 37, no. 2, p. 151-158. [\[CrossRef\]](#)
- SAWALHA, M.F.; PERALTA-VIDEA, J.R.; SAUPE, G.B.; DOKKEN, K.M. and GARDEA-TORRESDEY, J.L. (2007). Using FTIR to corroborate the identity of functional groups involved in the binding of Cd and Cr to saltbush (*Atriplex canescens*) biomass. *Chemosphere*, vol. 66, no. 8, p. 1424-1430. [\[CrossRef\]](#)
- SENTHILKUMAR, R.; VIJAYARAGHAVAN, K.; THILAKAVATHI, M.; IYER, P.V.R. and VELAN, M. (2006). Seaweeds for the remediation of wastewaters contaminated with zinc(II) ions. *Journal of Hazardous Materials*, vol. 136, no. 3, p. 791-799. [\[CrossRef\]](#)
- SINGH, A.; KUMAR, D. and GAUR, J.P. (2012). Continuous metal removal from solution and industrial effluents using *Spirogyra* biomass-packed column reactor. *Water Research*, vol. 46, no. 3, p. 779-788. [\[CrossRef\]](#)
- ULUÖZLÜ, Ö.D.; SARI, A.; TUZEN, M. and SOYLAK, M. (2008). Biosorption of Pb(II) and Cr(III) from aqueous solution by lichen (*Parmelina tiliaceae*) biomass. *Bioresource Technology*, vol. 99, no. 8, p. 2972-2980. [\[CrossRef\]](#)
- WILSON, D.; DEL VALLE, M.; ALEGRET, S.; VALDERRAMA, C. and FLORIDO, A. (2012). Potentiometric electronic tongue-flow injection analysis system for the monitoring of heavy metal biosorption processes. *Talanta*, vol. 93, p. 285-292. [\[CrossRef\]](#)
- YAHYA, S.K.; ZAKARIA, Z.A.; SAMIN, J.; RAJ, A.S.S. and AHMAD, W.A. (2012). Isotherm kinetics of Cr(III) removal by non-viable cells of *Acinetobacter haemolyticus*. *Colloids and Surfaces B: Biointerfaces*, vol. 94, p. 362-368. [\[CrossRef\]](#)

- YUN, Y.S.; PARK, D.; PARK, J.M. and VOLESKY, B. (2001). Biosorption of trivalent chromium on the brown seaweed biomass. *Environmental Science & Technology*, vol. 35, no. 21, p. 4353-4358. [\[CrossRef\]](#)
- ZHANG, Y. and BANKS, C. (2006). A comparison of the properties of polyurethane immobilised *Sphagnum* moss, seaweed, sunflower waste and maize for the biosorption of Cu, Pb, Zn and Ni in continuous flow packed columns. *Water Research*, vol. 40, no. 4, p. 788-798. [\[CrossRef\]](#)

#### How to reference this article:

PLAZA CAZÓN, J.; VIERA, M. and DONATI, E. (2013). Dynamic Cr(III) uptake by *Macrocystis pyrifera* and *Undaria pinnatifida* biomasses. *Electronic Journal of Biotechnology*, vol. 16, no. 3. <http://dx.doi.org/10.2225/vol16-issue3-fulltext-8>